

Simplified Pushover Analysis of Moment Resisting Frame Structures

Timothy J. Sullivan, Daniel Saborio-Romano, Gerard J. O'Reilly, David P. Welch & Luca Landi

To cite this article: Timothy J. Sullivan, Daniel Saborio-Romano, Gerard J. O'Reilly, David P. Welch & Luca Landi (2018): Simplified Pushover Analysis of Moment Resisting Frame Structures, Journal of Earthquake Engineering

To link to this article: <https://doi.org/10.1080/13632469.2018.1528911>



Published online: 14 Dec 2018.




Submit your article to this journal [↗](#)



View Crossmark data [↗](#)



Simplified Pushover Analysis of Moment Resisting Frame Structures

Timothy J. Sullivan, Daniel Saborio-Romano, Gerard J. O'Reilly , David P. Welch, and Luca Landi

University of Canterbury, QuakeCoRE, Christchurch, New Zealand

ABSTRACT

Seismic assessment of a building will typically require consideration of its nonlinear force–displacement response. Such information can be estimated from pushover analysis, also referred to as nonlinear static analysis, in which the structure is analyzed for incrementally increasing lateral loads and the nonlinear structural behavior is accounted for during the analysis by updating the stiffness matrix at each load increment. A number of computer programs are now available to permit the application of pushover analysis in practice. However, it is argued that there is a need for simplified pushover analysis methods to permit independent checks of computer outputs and also to inform engineers of the key characteristics of the structural system being assessed. This work builds on previous contributions in the literature to provide a simplified pushover analysis approach for reinforced concrete (RC) frame structures. A novel procedure for the assessment of the displacement profile of RC frames is provided, with guidelines to account for different types of yielding mechanisms. By comparing force–displacement response predictions with those obtained from rigorous nonlinear static analyses for a range of frame configurations and mechanisms, it is shown that the proposed approach offers an effective means of undertaking simplified pushover analysis.

ARTICLE HISTORY

Received 31 March 2018
Accepted 23 September 2018

KEYWORDS

Pushover Analysis;
Simplified Pushover
Analysis; Nonlinear Static
Analysis; Reinforced
Concrete Frames; Seismic
Assessment

1. Introduction

Nonlinear static analysis, often referred to as pushover analysis, is being used increasingly for the seismic assessment of structures, possibly because it offers a useful means of identifying weak links in a structure [Hall, 2017] and because a number of codes and guidelines have indicated it as a preferred assessment procedure [EN 1998-3:2005, 2005; NZS 1170.5:2004, 2004]. In order to undertake pushover analysis of a multistory frame structure, a set of lateral loads is increased in small steps with internal member forces and deformations computed at each load increment. Different options exist for the definition of the lateral load distribution, with triangular and uniform lateral load patterns prescribed within Eurocode 8 [EN 1998-1:2004, 2004] in addition to loading profiles that are updated incrementally as part of a more accurate adaptive pushover analysis [Antoniou and Pinho, 2004]. Nonlinear structural behavior, such as local yielding of beams or columns, can be accounted for during the analysis by updating the stiffness matrix at

CONTACT Timothy Sullivan  timothy.sullivan@canterbury.ac.nz

Color versions of one or more of the figures in the article can be found online at www.tandfonline.com/ueqe.

each load increment. In addition to obtaining useful information on internal forces and displacements, the results of the analysis can be transformed into an equivalent single-degree-of-freedom (SDOF) force–displacement plot that enables more simplified seismic assessment using procedures such as the capacity spectrum method [Freeman, 1978], the N2 method [Fajfar, 2000], or displacement-based assessment (DBA) [Priestley *et al.*, 2007]. Detailed descriptions and evaluations of different options for pushover analyses are provided in FEMA [440, 2005], Papanikolaou *et al.* [2006], and Pinho *et al.* [2006].

A number of computer programs, such as SAP2000 [CSI, 2000], Seismostruct [Seismosoft, 2014], Ruaumoko [Carr, 2007], and OpenSees [McKenna *et al.*, 2010], are now available to permit the application of pushover analysis in practice. However, engineers should always check the results obtained from a computer analysis model. An apparent difficulty with checking the nonlinear structural analysis of a multi-degree-of-freedom (MDOF) system is that one should arguably be prepared to form a large stiffness matrix and undertake numerous calculation steps, making this process impractical in the design office.

In light of the above, the objective of this paper is to further develop and test a simplified pushover analysis procedure for moment resisting frame structures that can be used to validate the results of a computer-based pushover analysis. It is also argued that by developing a simplified mechanics-based method for pushover analysis engineers may gain a better understanding of the key characteristics of a structure than they do from computer analysis alone. The method will build on the findings and recommendations from a number of previous contributions to the subject, where the work by Priestley and Calvi [1991] for the assessment of reinforced concrete (RC) frames is of particular relevance. Priestley and Calvi [1991] proposed a two-level approach in which capacity design principles [Park and Paulay, 1975] were first applied in reverse so as to identify the likely collapse mechanism. Strength and ductility capacity estimates for the system were then combined to provide an equivalent elastic response force level that was then used together with design response spectra to identify the annual probability of exceeding the structural capacity. Priestley [1997] developed this procedure further, emphasizing the importance of assessing the displacement response rather than force levels, and developing a so-called displacement-based seismic assessment approach. In doing so, Priestley [1997] proposed a number of simplified displacement profiles with which to establish an equivalent SDOF system for RC frames, illustrated in Fig. 1b, to be selected according to the expected mechanism (Fig. 1a) and number of stories, n , in the building.

As seen in Fig. 1, for an RC frame with a column-sway (soft-story) mechanism, the deformations are assumed to be concentrated at the soft-story level, with the stories above translating like a rigid body for a total system displacement capacity of $\Delta_{\text{sys,col}}$. For a beam-sway mechanism, more linear displacement profiles were suggested and Priestley [1997] provided equations for an equivalent SDOF system displacement, Δ_{sys} , as a function of the story drift demand at the base. The following equations for the full displacement profile, Δ_i , were later advocated for assessment by Priestley *et al.* [2007]:

$$\text{for } n \leq 4: \quad \Delta_i = \theta_c h_i \quad (1a)$$

$$\text{for } n > 4: \quad \Delta_i = \theta_c h_i \cdot \left(\frac{4H_n - h_i}{4H_n - h_1} \right) \quad (1b)$$

where θ_c is the critical (maximum) story drift (at ground level), h_i is the height of level i above the base, H_n is the total height of the structure, and h_1 is the first-floor height. This is an empirical expression verified through non-linear dynamic analyses of RC frame structures by Pettinga and Priestley [2005], amongst others. Note that the precise form of Eq. (1b) is taken from the model design code proposed by Sullivan *et al.* [2012] but it gives the same displacement profile as the expression presented within Priestley *et al.* [2007].

With the displacement profile of an MDOF system known, an equivalent SDOF system displacement, Δ_{sys} , effective mass, m_e , and effective height, H_e , can be computed according to the substitute structure approach [Gulkan and Sozen, 1974; Shibata and Sozen, 1976], illustrated in Fig. 1c. Subsequently, by plotting V_b versus Δ_{sys} , the pushover force-displacement curve for the equivalent SDOF system is obtained, such as that shown in Fig. 1d. The pushover curve could be used to validate results of a pushover analysis conducted in a computer or for simplified seismic assessment in accordance with the detailed seismic assessment guidelines of the New Zealand Society for Earthquake Engineering [NZSEE, 2017].

The overview provided above shows that some useful guidance for simplified pushover analysis of RC frames already exists. However, displacement profiles for RC frames are estimated using a limited number of expressions that are based either on simplistic reasoning or results of nonlinear dynamic analyses of a set of case study buildings. Unfortunately, as will be demonstrated later in Section 3.2, the existing expressions for displaced shape can lead to significant errors in the estimation of system displacement capacity and hence seismic risk. For example, it will be demonstrated later in Section 3.2 that adoption of Eq. (1) overestimates the displacement capacity of a real six-story RC frame building by as much as 34%. Consequently, the main focus of this paper is to

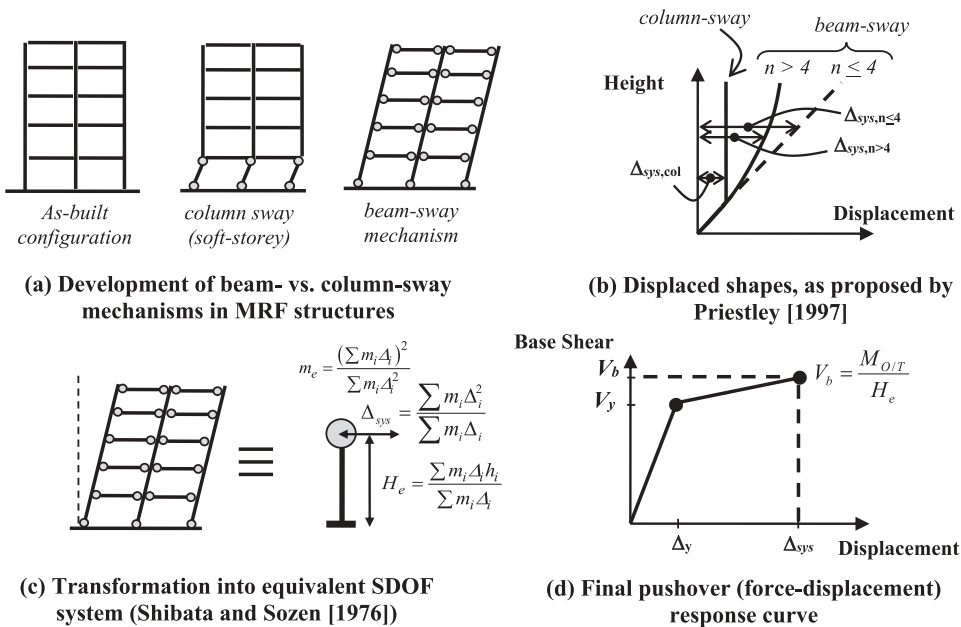


Figure 1. Overview of the displacement-based assessment procedure of Priestley *et al.* [2007].

develop and test an improved mechanics-based procedure for estimating the lateral displacement profile of moment-resisting frame structures, providing guidelines that cover a range of mechanisms that may potentially develop. To do this, the means of identifying the likely yield mechanism and resistance of beam-column sub-assemblages will first be reviewed. After then presenting a new procedure for estimation of shear and displacement profiles that should be comparable to those that would be obtained from pushover analyses, a number of case study buildings are used to illustrate the method's potential and gauge the likely benefits it offers over the existing simplified guidelines.

2. Proposed Procedure for Simplified Pushover Analysis of RC Frames

2.1. Assessing the Likely Mechanism and Lateral Resistance of Each Story

In the assessment procedure proposed by Priestley and Calvi [1991], the relative strengths of adjoining members are compared in order to identify the weakest element and action, which indicates the likely mechanism. To illustrate this, consider the two-story RC frame structure shown in Fig. 2.

Beginning, for this example, with the left beam at the first floor of the frame, one could first hypothesize that beam flexural hinges could form at either end of the beam. In line with this, the bending moments, M_{bl} and M_{br} , are computed, corresponding to the section resistances at the column faces of the left and right end of the beams, respectively, as indicated in Fig. 2a. The bending moments at any point along the beam should then be calculated, making due allowance for the uniformly distributed gravity load, w , and any anticipated vertical earthquake acceleration demands. If the beam flexural resistance were to be inferior to the flexural demands at any intermediate point along the beam, then the location of the expected hinges would need to be revised and the bending moment profile recomputed.

The development of a flexural mechanism in the beam will only be possible if the beam is able to sustain the shear forces associated with the flexural hinging. This is usually assured through capacity design but for existing RC frames, there is a possibility of premature shear failure and so it should be checked. This is done by computing the shear resistance of the beam, V_{Rb} , and comparing this with the shear demand, V_{Db} ,

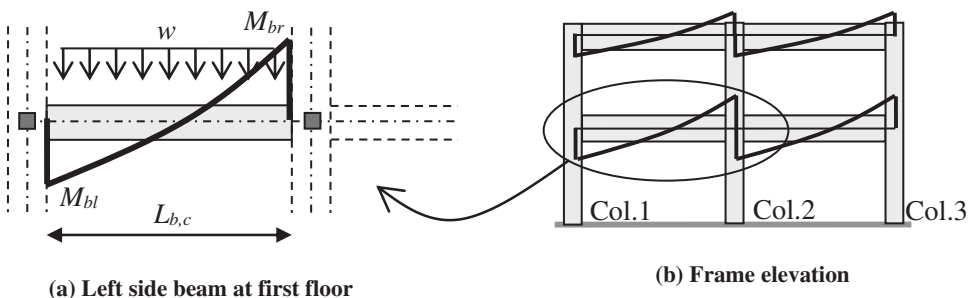


Figure 2. Investigating the likely mechanism in a two-story RC frame.

expected in the beam if a beam flexural mechanism were to form; calculated for the right-hand side of the beams shown in Fig. 2a as follows:

$$V_{Db} = \frac{M_{bl} + M_{br}}{L_{b,c}} + \frac{wL_{b,c}}{2} + V_{vEQ} \quad (2)$$

where $L_{b,c}$ is the clear length of the beam between columns as indicated in Fig. 2a, $V_{v,EQ}$ is the shear associated with vertical excitation component of ground motion (if deemed significant) and all the other symbols have been defined above. The magnitude of vertical accelerations will be uncertain, owing to uncertainty in the ratio of peak horizontal and vertical acceleration demands as well as the uncertain dynamic amplification of vertical acceleration demands up the height of a building. Clearly, if the purpose of these calculations is to assess the likely mechanism under lateral loading only, then $V_{v,EQ}$ could be set to zero. If V_{Db} is equal to or greater than V_{Rb} (the beam shear resistance), then a shear mechanism in the beam is likely to occur prior to a flexural mechanism. If instead V_{Db} is less than V_{Rb} , then the development of a flexural mechanism in the beam is more likely.

The process described above could be repeated for all beams in the frame such that the maximum beam end moments at all locations in the frame are identified. Subsequently, the column bending and shear capacities should be checked in a similar fashion. When computing section resistances for beams and columns, the impact of poor detailing, such as the presence of smooth reinforcement or inadequate lap splice details, should be accounted for following guidelines [Calvi *et al.* 2002a; Priestley *et al.* 1996]. When computing the column section strengths, an important uncertainty will be the axial load acting on the column during seismic loading, recognizing that, in addition to varying vertical acceleration demands, the beam shears induced by seismic loading will tend to increase axial loads on some columns (such as column 3 in Fig. 2b) and reduce them on others (such as column 1 in Fig. 2b). It is recommended that the column's strengths be computed initially assuming gravity-induced axial loads only. This is because, as argued by Priestley *et al.* [2007], the difference in total base shear resistance obtained with account for varying column axial loads will typically be negligible. However, local mechanisms (e.g. premature joint failures) can be affected and so once the base shear resistance has been computed, the axial forces due to seismic loading can be estimated, member strengths recalculated, and an iterative assessment process followed. Whether such a refined iterative assessment process is necessary will depend on the case at hand considering the potential impact on overall base shear estimates and displacement capacity.

Having computed both the maximum end moments for columns and beams, one then needs to establish whether beam or column hinging is most likely. This again refers to the application of capacity design principles in reverse, recognizing that in capacity design column flexural strengths are set as a function of beam flexural resistances in order to force a beam-sway mechanism to occur. As such, the sum of end moments of columns framing into a joint should be compared with those from beams (taking care to compare equivalent moments at joint centerlines as opposed to moments at plastic hinge locations) and the lower will indicate whether column or beam hinging can be expected. For example, Fig. 3a presents beam and column end moments at the centerlines of two joints in the two-story frame structure. It can be seen that the sum of column end moments (480 kNm) is greater than the beam end moment (200 kNm) for column 1. Hence, beam hinging is expected for this beam-column sub-assembly. In contrast, the sum of column

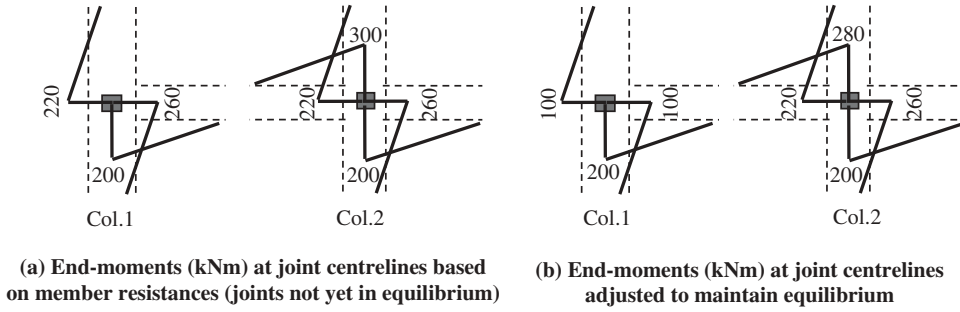


Figure 3. Adjusting beam and column end moments at first floor of two-story frame example.

end moments (480 kNm) is less than the beam end moments (500 kNm) for column 2, and hence, column hinging is expected for this beam–column sub-assembly.

In addition to comparing beam and column resistances, however, the beam–column joints themselves should be checked, following recommendations such as those provided in Priestley *et al.* [2007] and [Tasligedik *et al.*, 2018] as they may be weaker than the adjoining elements and hence would dictate the local mechanism. A final set of end moments in beams and columns, which accounts for beam, column, and joint resistances, should then be established that respects equilibrium. This will require redistribution of the mechanism joint moment to the adjoining members. The proportions of joint moment that will be distributed to adjoining elements will actually depend on their stiffness and strength. However, in order to avoid the need to compute member stiffnesses in this process, it is recommended that joint moments are initially split equally to adjoining members. In line with this, Fig. 3b shows that for column 1 the beam moment resistance of 200 kNm is split equally to the columns above and below the joint, which both remain elastic. For column 2, it can be seen that if the resisting moment of 480 kNm at the beam–column joint were split equally to the adjoining members (i.e. 240 kNm to each beam) then the beam on the right would be overloaded since it has a resistance of only 200 kNm. In such cases, the recommendation is to set the end moment in the right beam equal to its resistance (i.e. 200 kNm) and then redistribute the remaining moment demand to the other beam (such that it carries a total demand of 280 kNm).

Upon completion of the process described above, column end moments will have been identified for all beam–column joint regions in the frame. These end moments can then be used to compute values of story shear resistance, by summing up the column shears for each story, as follows:

$$V_{R,i} = \frac{\sum M_{col,b,i} + \sum M_{col,a,i-1}}{(h_i - h_{i-1})} \quad (3)$$

where $V_{R,i}$ is the shear resistance of story i and, h_i and h_{i-1} are the heights above the base foundation of levels i and $i-1$ respectively. The terms $\sum M_{col,b,i}$ and $\sum M_{col,a,i-1}$ are the sum of the column end moments immediately below the joint centerlines at level i and above the joints at level $i-1$, respectively. This equation thus assumes that the joint centerlines at a given level are all at the same height. For the first story it is clear that h_{i-1} should be set to zero whereas the term $\sum M_{col,a,i-1}$ should be taken equal to the column base moment

capacities (which may need to be set as a function of column shear capacity if a column were not to have sufficient shear strength to support the development of flexural hinges).

2.2. Assessing the Drift Required to Yield Each Story

Recognizing that the pushover procedure will provide information on both the forces and displacements that develop in a structure, attention is now turned to the drift that is required to cause an RC frame to yield. Equations (4)–(8) provide a series of approximate mechanics-based expressions for the drift at yield of level i in an RC frame as a function of the expected mechanism.

$$\text{For beam – sway flexural mechanisms: } \theta_{y,i} = 0.5 \frac{\varepsilon_y L_{b,i}}{h_{b,i}} = \theta_{y,bs,i} \quad (4)$$

$$\text{For column – sway flexural mechanisms: } \theta_{y,i} = 0.43 \frac{\varepsilon_y h_{s,i}}{D_{col,i}} = \theta_{y,cs,i} \quad (5)$$

$$\text{For beam – column joint mechanisms: } \theta_{y,i} = \frac{M_{j,joint,i}}{M_{j,beams,i}} \theta_{y,bs,i} \quad (6)$$

$$\text{For beam shear mechanisms: } \theta_{y,i} = \frac{L_{b,c,i} (V_{Rb,i} - 0.75wL_{b,c,i})}{M_{bl,i} + M_{br,i}} \theta_{y,bs,i} \quad (7)$$

$$\text{For column shear mechanisms (no in fills): } \theta_{y,i} = \frac{V_{R,i}}{V_{R,i,cs}} \theta_{y,cs,i} \quad (8)$$

where ε_y is the yield strain of the longitudinal reinforcement in the beams, $L_{b,i}$ is the length of the beams between column centers, $h_{b,i}$ is the section depth of the beams, $h_{s,i}$ is the story height (between floor centerlines), $D_{col,i}$ is the column section depth, $M_{j,joint,i}$ is the beam–column joint equivalent moment capacity, $M_{j,beams,i}$ is the total flexural resistance of beams framing into a beam–column joint (see earlier discussion with reference to Fig. 3), $L_{b,c,i}$ is the length of the beams between column faces, $M_{bl,i}$ and $M_{br,i}$ correspond to the beam section resistances at the left and right end of the beams (see earlier discussion with reference to Fig. 2), $V_{Rb,i}$ is the beam shear resistance, $0.75wL_{b,c,i}$ represents the beam shear demand associated with gravity loading and vertical excitation (see earlier discussion with respect to Eq. (2)), $V_{R,i}$ is the story shear resistance associated with a column shear failure, and $V_{R,i,cs}$ is the story shear resistance computed assuming that a column-sway flexural mechanism could form (see earlier discussion with respect to Eq. (3)).

Priestley *et al.* [2007] proposed Eq. (4) as a means of estimating the yield drift of a well-detailed RC frame in which a flexural mechanism is expected to form. The equation was set by making estimates of the different contributions to yield drift of a frame and was verified using experimental results collected from the literature. Equation (5) was formulated by Glaister and Pinho [2003] along similar lines, making estimates of beam, joint, and column-shear deformations relative to the column flexural deformations. Equation (6) proposes that the drift at formation of a beam–column joint mechanism can be found by simply scaling the yield drift associated with a beam-sway flexural mechanism (i.e. Eq. (4)) by the ratio of the force required to form a beam–column joint mechanism to the force

that would have been required to form a beam-sway flexural mechanism. Similarly, Eqs. (7) and (8) are scaling the yield drifts associated with flexural sway mechanisms by the ratio of the shear resistance available against seismic loading to the shear demand that would be expected if the associated flexural sway mechanism were to develop. Note that the drift predicted by Eq. (8) presumes that masonry infills are not present as these will tend to increase both stiffness and shear demands on columns in RC frames, subsequently affecting yield drifts. To the authors' knowledge, Eqs. (5)– (8) have not been verified experimentally and may need to be revised as part of future research. However, they are recommended for the purposes of simplified pushover analysis until more refined expressions become available. Also, note that no allowance has been made for the effects of smooth reinforcement or lap-splice problems, but this is considered outside the scope of the current paper.

At the base of an RC frame, the drift required to yield the cantilever RC columns should also be estimated. For columns yielding in flexure, this can be done via the relevant form of Eq. (9). Note that in the event that a shear mechanism is expected in the columns at the ground story the yield drift should instead be computed according to Eq. (8).

$$\text{For rectangular ground – storey columns : } \theta_{y,0} = 0.70\varepsilon_y \frac{h_{cf}}{D_{col}} \quad (9a)$$

$$\text{For circular ground – storey columns : } \theta_{y,0} = 0.75\varepsilon_y \frac{h_{cf}}{D_{col}} \quad (9b)$$

where D_{col} is the column section depth (outside diameter in the case of circular sections) in the direction of loading, and h_{cf} is the height of contraflexure expected in the ground story column that can be estimated as follows:

$$h_{cf} = \frac{h_1}{\left(\frac{M_{col,b,1}}{M_{col,base}} + 1\right)} \quad (10)$$

where, as shown in Fig. 4, h_1 is the first story height, $M_{col,b,1}$ is the moment expected to develop at the top of the column (just below the beam–column joint centerline), and $M_{col,base}$ is the base flexural strength of the column. Figure 4 also illustrates the manner with which Eq. (9) has been derived, integrating the linear curvatures (approximated as varying linearly in

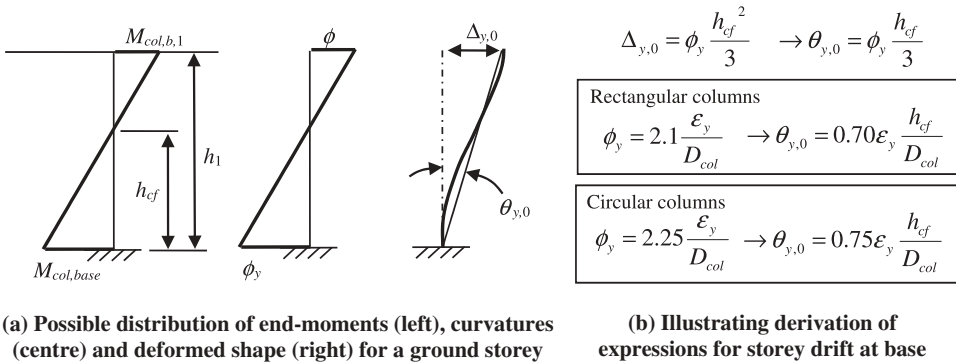


Figure 4. Yield drift considerations for ground story cantilever columns.

proportion to the moment demands) and adopting the nominal yield curvature expressions for RC columns provided by Priestley *et al.* [2007]. No allowance has been made for foundation flexibility, and if this were deemed significant, it should be added.

Up until this point in the paper, the term “story” and “level” could be seen as being somewhat equivalent. However, when undertaking structural analyses, the “story” drift demand is typically computed as the relative lateral displacements of adjacent “levels,” divided by the story height [O’Reilly *et al.*, 2017]. This is relevant because the yield drift expression given by Eq. (4) refers to beams at a certain level and Eq. (9) refers to the bases of ground story columns. Clearly, the yield drift of a “story” as opposed to a “floor” level will require that resistance has been developed at both the top and bottom of the story. In the case of the ground story, this could imply that flexural yielding needs to occur at the base of the columns and also at the ends of the beams of the first floor. At upper stories, it could imply yielding of beams at the levels above and below the story in question. To account for this, the yield drifts at each adjacent level can be weighted according to strain-energy proportions, as per Eq. (11):

$$\theta_{y,sys,i} = \frac{\sum M_{j,i} \theta_{y,i} + \sum M_{j,i-1} \theta_{y,i-1}}{\sum M_{j,i} + \sum M_{j,i-1}} \quad (11)$$

where $\theta_{y,sys,i}$ is the story drift required to yield story i , $M_{j,i}$ and $M_{j,i-1}$ are the total flexural resistances (for the governing mechanism) provided at joint centers, and $\theta_{y,i}$ and $\theta_{y,i-1}$ are the drifts at yield at levels i and $i-1$ respectively. Note that the summation terms are indicated since it is expected that at a given level there will be a number of beam–column joints (in multiple frames) providing resistance against lateral movement of that level. At the ground story $i = 1$, $M_{j,0}$ would correspond to the flexural strength and $\theta_{y,0}$ the yield drift of the column bases, found in line with guidelines provided above.

Typically, the above distinction between “story” and “floor” level drift is not made (as, for instance, in Priestley *et al.* [2007]) since the differences that result in design are not significant. However, the authors have found that for pushover assessment of existing frames, such a rigorous evaluation of the story drift can be useful in understanding the mechanism that forms and correctly predicting the nonlinear response that develops.

2.3. Assessing Values of Story Stiffness

Having found means of identifying the story shear resistance (Eq. (3)) and story drift at yield (Eq. (11)), the secant stiffness to yield, $k_{y,i}$, at each story i can now be computed as follows:

$$k_{y,i} = \frac{V_{R,i}}{\theta_{y,i} h_{s,i}} \quad (12)$$

where all symbols have been defined in previous sections. The story stiffness values so defined are useful for calculation of elastic inter-story displacement components along the height of the frame, as will be explained in the next section.

2.4. Assessing Displacement and Story Shear Profiles

The purpose of this paper is to provide a simplified means of undertaking pushover analyses of RC frames, which essentially requires the ability to identify the lateral displaced shape and story shear demands for various levels of roof displacement or base shear. The information derived in the preceding sections can be used for such pushover analyses by following the general procedure outlined in Fig. 5. The details of each step will be explained in the paragraphs that follow.

In the first step of the procedure, an estimate of the base shear at yield of the frame is made. This estimate will be checked and revised during the assessment procedure and hence the exact value is not too important, but a useful starting point may be to assume that the base shear at yield of the frame would be equal to the story shear resistance at the ground floor, found from Eq. (7) with $i = 0$.

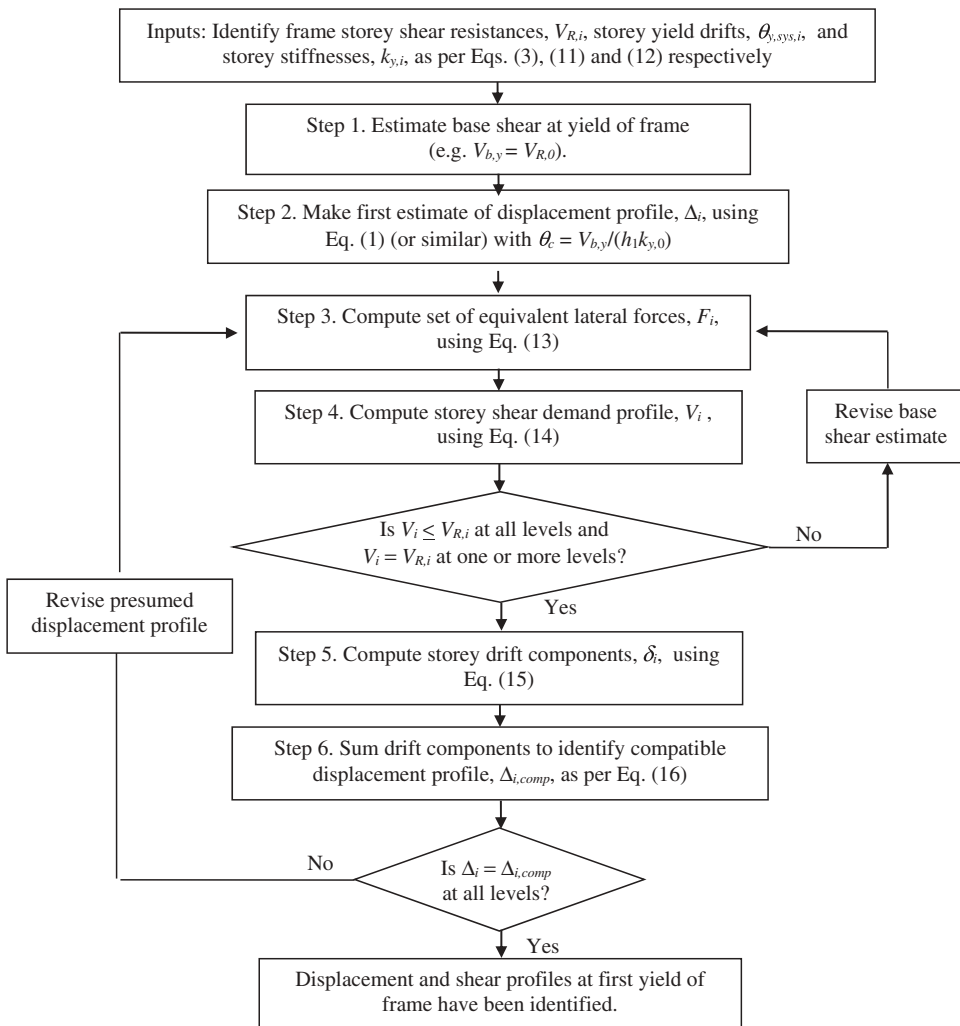


Figure 5. Procedure to identify displacement and shear profiles at yield of RC frame.

A trial displacement profile for the frame is set at step 2, and for this purpose it is suggested that Eq. (1) be used, with the drift at ground story, θ_c , obtained by dividing the yield base shear by the ground story stiffness, $k_{y,0}$ (from Eq. (12)) and height, h_1 .

In step 3, a set of equivalent lateral forces, F_i , is found according to Eq. (13) from Priestley *et al.* [2007]:

$$F_i = \frac{m_i \Delta_i}{\sum m_i \Delta_i} V_b \quad (13)$$

where V_b is the frame base shear force (noting that $V_b = V_{b,y}$ at first yield of the frame), m_i is the seismic mass, and Δ_i the lateral displacement of level i .

In step 4, the story shear demands associated with V_b are then found by summing the equivalent lateral forces from Eq. (13) down the height of the n -story frame, from levels n to i , according to

$$V_i = \sum_{j=i}^n F_j \quad (14)$$

At this point in the procedure, the shear demands should be compared with the shear resistances for each story. Ideally, the shear demand will be equal to the shear resistance at one or more stories and should nowhere exceed the shear resistance. If the demand exceeds the resistance at any story, then the estimated base shear at yield of the frame was too high, a reduced base shear estimate should be made, and the procedure repeated from step 3. On the other hand, if the shear demands are less than the shear capacities at all levels, this suggests that the yield base shear was too low and hence, an increased estimate should be made and the procedure repeated from step 3.

At step 5, elastic story drift components are found by dividing the story shear demands by the story shear stiffness values, $k_{y,i}$ (found from Eq. (12)), according to

$$\delta_i = \frac{V_i}{k_{y,i}} \quad (15)$$

In step 6, the lateral displacement profile, $\Delta_{i,comp}$ that is expected to be compatible with the base shear is computed by summing the drift components up the height of the frame, according to

$$\Delta_{i,comp} = \sum_{j=1}^i \delta_j \quad (16)$$

The displacement profile computed according to Eq. (16) should then be compared with the displacement profile assumed at step 2. If the displacements do not match, a revised estimate of the displacement profile should be made (and it is recommended that the revised estimate be set equal to the displacements computed by Eq. (16)) and the assessment procedure repeated from step 3. If the displacement profiles match, the procedure is complete and the story shear and lateral displacements at yield of the frame have been found.

2.5. Assessing the Global Post-Yield Mechanism

Beyond yield, the deformed shape of the frame structure will depend on the mechanism that develops. The process described in Section 2.1 will have indicated the sort of mechanism that is expected at a beam–column sub-assembly level, recalling that one might identify either flexural beam- or column-hinging, joint-hinging, or shear failures of beam or column elements. Knowing also the story at which yielding is first expected to develop (from the procedure just described in the previous section) one may be in a position to anticipate the global mechanism too. For example, if column flexural hinging is assessed for the sub-assemblies of the story at which the shear resistance is first reached (i. e. the story where $V_i = V_{R,i}$ according to the process described in Fig. 6), then a global soft-story mechanism at this level will develop and plastic deformations will concentrate at the soft-story level (see Fig. 2a). If, however, flexural beam hinging is assessed at the sub-assembly level then one could anticipate that a beam-sway mechanism will begin to develop, in which deformations increase gradually at all levels (again see Fig. 2a).

In some cases, a mixed mechanism might be expected, whereby some beam–column sub-assemblies at a level will have been assessed as, say, column-sway critical whereas other sub-assemblies may be beam-sway. In such cases one might expect the same result as a beam-sway mechanism, with deformation demands spreading over the height of the building. However, some judgment may be required since the capacity to redistribute loads will depend on the number and relative resistance of those columns not expected to yield. Priestley *et al.* [1991] and Priestley *et al.* [2007] recommend that a sway potential index, S_i , be calculated for each floor to indicate the likelihood of a column-sway mechanism.

$$S_i = \frac{\text{sum of beam strengths at level } i}{\text{sum of column strengths at level } i} \quad (17)$$

When S_i is greater than 1.0, a column-sway mechanism is expected. When S_i is less than 1.0, a beam-sway mechanism could be expected, but Priestley *et al.* [2007] point out that if S_i is greater than 0.85 then it would be reasonable to assume (in an effort to be conservative) that a column-sway mechanism may develop. However, this expression is not likely to capture those cases with unusual distributions of beam and column strengths. In addition, Sullivan and Calvi [2011] point out that for older buildings one might obtain sway potential indices greater than 1.0 at more than one level and hence be unsure about where the soft-story should be expected. To overcome this, Sullivan and Calvi [2011] proposed a sway-demand index, S_{Di} , as follows:

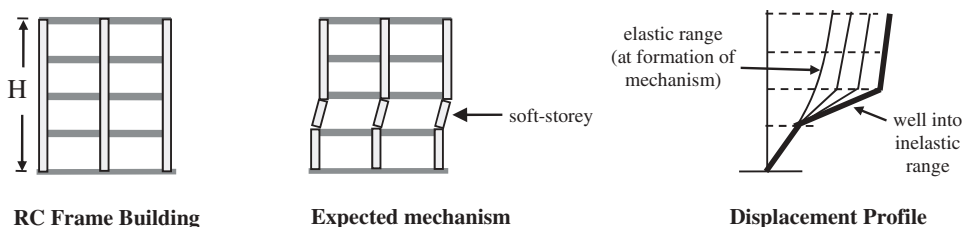


Figure 6. Illustrating potential impact of soft-story mechanism on lateral displacement profiles.

$$S_{Di} = \frac{\text{storey } i \text{ shear demand}}{\text{storey } i \text{ shear resistance}} = \frac{V_i}{V_{R,i}} \quad (18)$$

The story with the greatest value of SD_i for which column- (or joint) hinging is expected will indicate the story most likely to form a soft-story mechanism. Note that by following through the process described in Fig. 6 one will have evaluated both V_i and $V_{R,i}$ and hence will be able to calculate sway-demand indices easily.

Another complex scenario arises when one expects a beam-sway mechanism to begin at one level but then a column-sway mechanism is expected at another. In such cases, the drift profile found from the process described in Fig. 6 can be uniformly amplified until the drift reaches yield at a column-sway level, from which point a column-sway deformed shape could be assumed. This sort of scenario is difficult to predict via simplified methods as there is likely to be some redistribution of moments going to columns above and below joint centerlines, such that the shear resistance of different stories changes with increasing drifts and this in turn means that a soft-story can eventually develop even if the shear demands expected from the first-yield assessment process in Fig. 6 might not have indicated this.

2.6. Assessing the Displacement and Shear Profiles Post Yield

With knowledge of the displacement and shear profiles at yield of the RC frame, displacement and shear profiles at other post-yield states can also be derived. The means of doing this will be different for different sway mechanisms; for a beam-sway mechanism it is proposed that the displaced shape obtained from the procedure described in Fig. 5 be uniformly scaled until a target value of story drift is achieved. For a column-sway mechanism, it is instead expected that post-yield, deformations tend to concentrate at the soft-story level as shown in Fig. 6. As such, in this case the drift component, θ_i , at the soft-story level should be increased until a target drift level of interest is achieved, and then a revised displacement profile established according to Eq. (16). The changing displaced shape associated with the soft-story mechanism will change the distribution of equivalent lateral forces (as per Eq. (13)), with the tendency being for the levels above the soft-story to deform less. An iterative approach could be used to account for this changing displaced shape, but it will typically be sufficient to presume that the levels above the soft-story maintain drifts similar to those at formation of the mechanism, as indicated in Fig. 6.

For the case that an RC frame is expected to develop beam–column joint hinging, there is uncertainty as to the likely displaced shape. This is because, as pointed out by Calvi *et al.* [2002b], and others, joint shear hinges may form across two stories, rather than top and bottom of a single story. A conservative approach in this case might be to assume that the soft-story does form at a single story (since the global deformation capacity will be less in this case) but it is acknowledged that this is an area requiring further research.

3. Validation of the Simplified Approach

To gauge the validity of the simplified procedure described in the previous section, a series of case study applications have been made and the results obtained from accurate non-linear static analysis procedures are compared with those obtained from the simplified approach and previous recommendations in the literature. The potential benefits of the new approach will become clear in the subsections that follow.

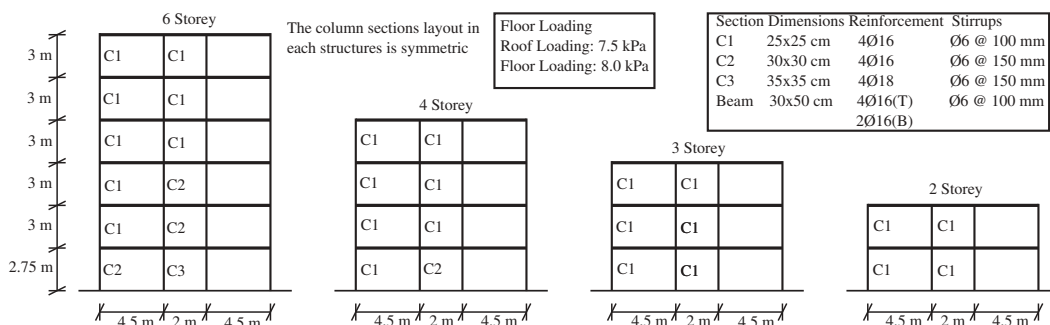


Figure 7. Layout of 2D case study structures adopted from Galli [2006].

3.1. Assessing Lateral Force–Displacement Profiles for a Series of 2D RC Frames

The first of these case study buildings consist of a series of 2D RC frames with different story number and are shown in Fig. 7. The designs are adapted from a previous study by Galli [2006] and have been designed for gravity load only using allowable stress and other such design provisions specified in Regio Decreto 2229/39 [Regio Decreto, 1939], along with other common construction conventions prior to the introduction of seismic design provisions in Italy in the 1970s, which are summarized in Vona and Masi [2004]. A common feature of these older frames is the absence of capacity design considerations in the beam and column members meaning that non-ductile mechanisms such as column-sway mechanisms are quite typical. Column members in these older frames typically possess low ratios of longitudinal reinforcement ($< 1.3\%$) as they were sized for axial loading and the use of smooth reinforcing bars was also common. The use of these bars in place of modern ribbed bars affects the bonding of the reinforcement to the concrete paste, resulting in a modified hysteretic behavior, as discussed in O’Reilly and Sullivan [2017]. Experimental testing by Pampanin *et al.* [2002] also showed how the small percentage of shear reinforcement stirrups in the members and no reinforcement in the beam–column joints meant that they are quite vulnerable to a non-ductile mechanism when combined with the use of smooth end-hooked bars.

The layout and various details regarding the member cross sections of the case study structures are shown in Fig. 7 where the column section sizes remain constant for the two- and three-story frames and the lower levels have slightly larger sections in the four- and six-story frames. The strength of the reinforcing steel and concrete was 3800 kg/cm^2 (372 MPa) and 200 kg/cm^2 (19.6 MPa), respectively, as per typical design manuals in use at the time of construction. In terms of numerical modeling the case study frames, the developments of O’Reilly and Sullivan [2017] were utilized herein for the structures and further details regarding the characterization of the response of these frames can be found in O’Reilly and Sullivan [2018].

The static pushover (SPO) analyses were conducted and four limit states corresponding to those described in the Italian National code [NTC, 2008] were identified for each structure in O’Reilly and Sullivan [2017b]. These limit states can be qualitatively described as follows along with their respective abbreviations listed in [NTC, 2008]: operational (SLO), damage control (SLD), life safety (SLV), and collapse prevention (SLC). Figure 8 shows the comparison between the four case study frames at each of these four limit states normalized to the roof displacement. As is evident, the simplified procedure outlined here provides an excellent match for each limit

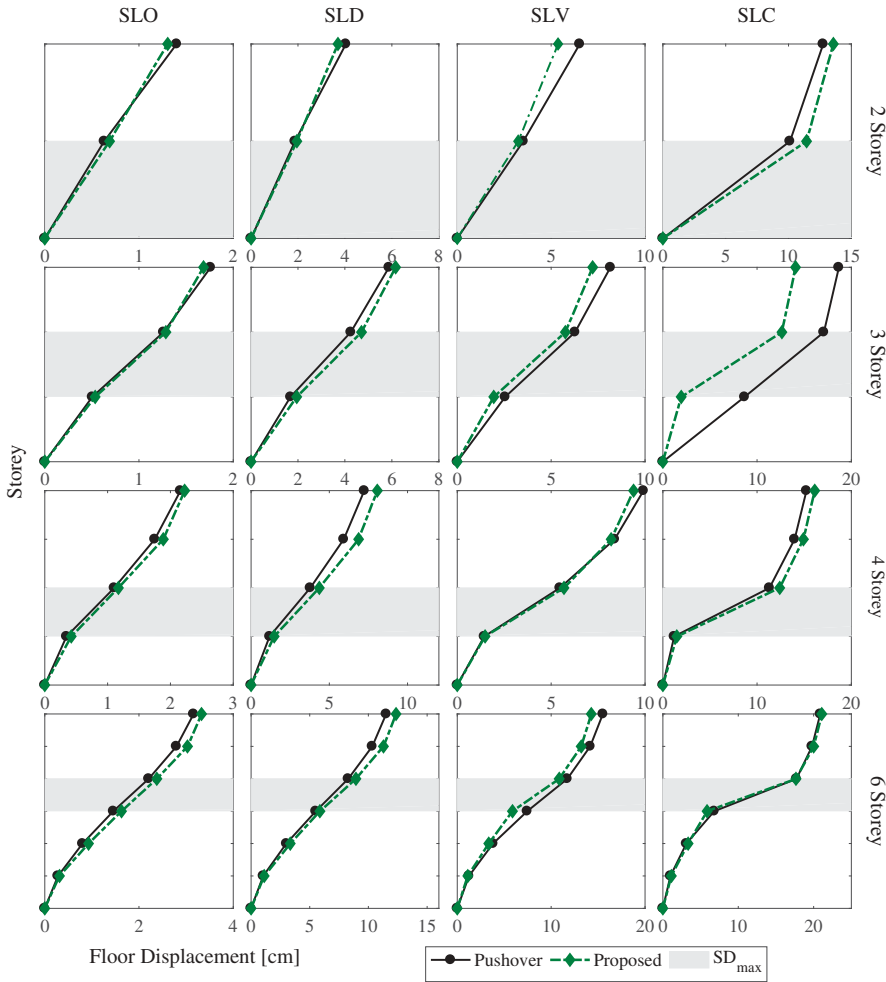


Figure 8. Comparison of the normalized displaced shape expression with the SPO analyses at various limit states.

state. The initial elastic behavior of the frames described via the elastic first mode shape in Fig. 8 is seen to be well represented by the proposed procedure followed by the gradual evolution of the plastic mechanism in the nonlinear range of response. This is especially evident in the case of the six-story building in how the stiffness of the lower floors is captured well in the elastic range of response and how the displaced shape moves gradually from the elastic first mode pattern to the concentration of damage on the fourth floor for the SLC limit state. The critical story predicted using the sway demand index in Eq. (18) is hatched in gray for each case study building in Fig. 9, where it can be seen that the approach was successful. This correct prediction of the story mechanism in each case provides further validation to the use of the sway demand index described in Section 2.5.

One instance where it is clear that more research is required, in terms of considering the beam–column joint mechanism’s influence on the distribution of drift between adjacent stories, is evident in the case of the three-story frame at the SLC limit state shown in Fig. 9. The procedure highlighted above determines that a soft-story

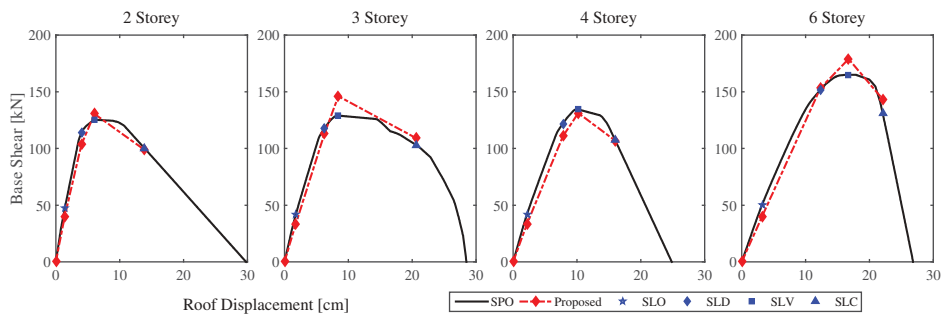


Figure 9. Comparison of the backbone response computed via the proposed procedure to that of static pushover (SPO) analysis.

mechanism forms at the second story of the building and when considering the comparison at the lower limit state SLV, it appears the method captures this well. However, at the final limit state SLC, the SPO has formed column base hinging together with a joint mechanism at the second floors, resulting in a spread in drift demand between these two floors.

Having determined the likely mechanism and associated displaced shape, the base shear associated with the anticipated mechanism at different levels of response can be computed to construct the overall backbone response curve of the building. That is, knowing that a column-sway mechanism will form, for example, the total base shear can be computed by estimating the story shear from the critical story along with the other relevant contributions to the total base shear from the other stories. The contributions from the other floors that are expected to remain elastic are determined as a ratio of the expected ductility demand, whereby using the yield drift approximation formula for a beam or column-sway, respectively, the expected ductility can be computed from the ratio of the limit state demand drift profile. Following this approach, the SPO curves for each of the case study frames are compared to the results of the proposed simplified approach at each of the four limit states and are illustrated in Fig. 9. This is performed by taking the critical drift associated with each limit state identified in O'Reilly [2016] and computing the base shear corresponding to the identified mechanism and overall displaced shape. Using the predicted base shear at each of the limit states and comparing them with those marked on the SPO curve, it can be seen that a good match is obtained. This is notable for the case of the operational limit state (SLO) in the initial elastic range and also in the drop in the base shear capacity at the collapse prevention limit state (SLC) of the structure where both strength degradation and the influence of P-Delta effects become more pronounced.

3.2. Assessing the Lateral Force–Displacement Profile for a Real Building in L'Aquila Italy

3.2.1. Overview

The assessment procedure has also been tested on an existing six-story building, consisting of multiple RC frames with unreinforced masonry partitions and infill walls located in the

Italian city of L'Aquila. The first story consists of a basement for storage and is separated from the perimeter retaining walls by a gap of 80 cm. The second story consists of offices, shops, and garages, and the last four stories are residential. The structure has seven bays in the east–west direction (X-direction) and three in the north–south direction (Y-direction), with a total area per story of 340.5 m², as shown in Fig. 10. The building is regular in plan, with the RC columns continuous along the height, while the masonry infill walls and partitions vary along height due to differences in architectural configurations. The frame sections (beams and columns) are gradually reduced from the lower to the upper stories in a somewhat conventional fashion. However, the story heights increase from the lower to the upper stories, causing a story stiffness irregularity along the height, with stiffer stories in the lower levels and more flexible in the upper levels.

In order to assess the appropriate displaced shape of RC frames only, the building was analyzed as bare frames, neglecting the contribution of the masonry infill walls in the structure capacity in this paper. To see the contribution of the masonry walls into the building capacity, see the results of Saborío-Romano [2016]. A three-dimensional structural model was created using the Ruaumoko 3D [Carr, 2007] software, where the RC columns and beams were modeled as lumped plasticity elements, allowing plastic hinges formation on both ends of the elements. The material properties and moment capacities used for this model were established and are detailed further in Saborío-Romano [2016].

3.2.2. Numerical Analysis

The structural model was subjected to both elastic modal and nonlinear SPO analysis. While the modal analysis provides the elastic dynamic properties of the structure, the pushover analysis characterizes the inelastic mechanism formation sequence and force–displacement relationship under increasing lateral forces. The results of the modal analysis are shown in Table 1, with mode shapes plotted in Fig. 12a. The first mode in each direction has the highest percentage of effective mass and so is taken as the fundamental natural period and mode shape. In addition, for this mode it can be seen that the structure seems to be stiffer in the first two stories of the structure, which is a reasonable result due to the increase in the story height and the reduction of the column section moving from the lower stories to the higher levels.

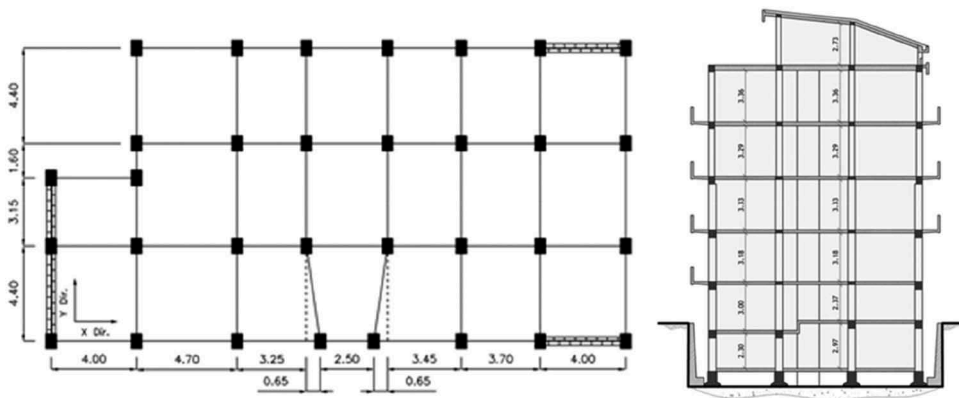
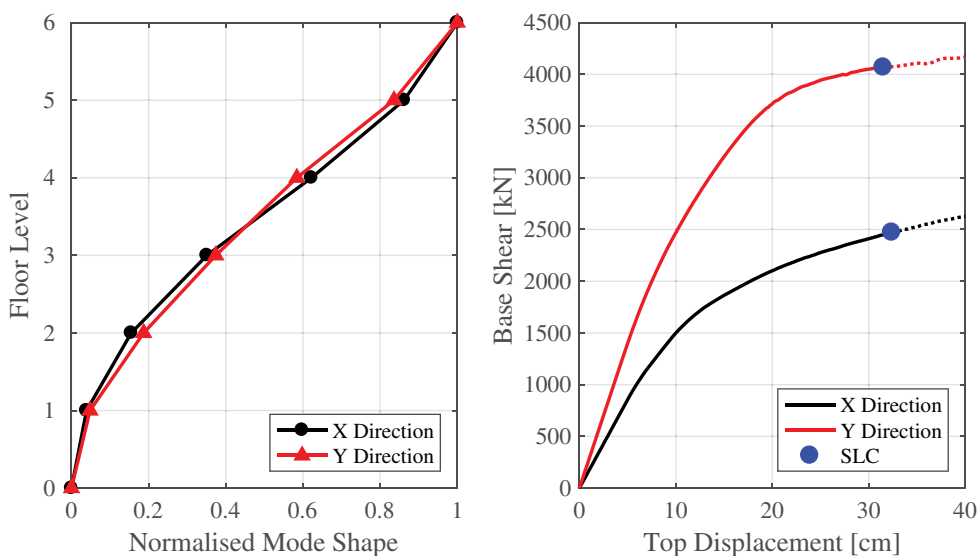


Figure 10. Plan view of the building (left) and transverse section (right) in the Y-direction, respectively, taken from Saborío-Romano [2016].

Table 1. Modal analysis results for the structural model, modified from Saborío-Romano [2016].

		X-direction		Y-direction	
		Mode 1	Mode 2	Mode 1	Mode 2
Period, T (s)		1.83	0.64	1.43	0.56
% Participating mass		66.1	15.4	64.1	13.7
Mode shape	Level 6	1.000	1.000	1.000	1.000
	Level 5	0.862	0.130	0.836	0.100
	Level 4	0.622	-0.703	0.584	-0.681
	Level 3	0.351	-0.865	0.374	-0.796
	Level 2	0.155	-0.525	0.187	-0.531
	Level 1	0.039	-0.153	0.048	-0.146

**Figure 11.** (a) First mode shapes and (b) force–displacement capacity curves for both analysis directions up to the collapse prevention (SLC) limit state, modified from Saborío-Romano [2016].

The pushover analysis was then performed using an inverse triangular load distribution for both principal directions of the building and results are shown in Fig. 11. The limit states were defined according to the Italian National Code [NTC, 2008] and correspond to: operational (SLO), damage control (SLD), life safety (SLV), and collapse prevention (SLC). The corresponding story drift capacities at the SLO, SLD, SLV, and SLC limit states were 0.33%, 0.50%, 2.0%, and 2.6%, respectively, for the X-direction and 0.33%, 0.50%, 2.0%, and 2.7%, respectively, for the Y-direction.

Comparing the capacity curves of Fig. 11, the structure is stiffer and stronger in the Y-direction for both models with respect to the X-direction, which is an expected result since all of the frames in the Y-direction have deep beams, whereas in the X-direction, the outer frames have deep beams and the interior frames have flat, shallow beams that were typical of older RC frame construction in Italy.

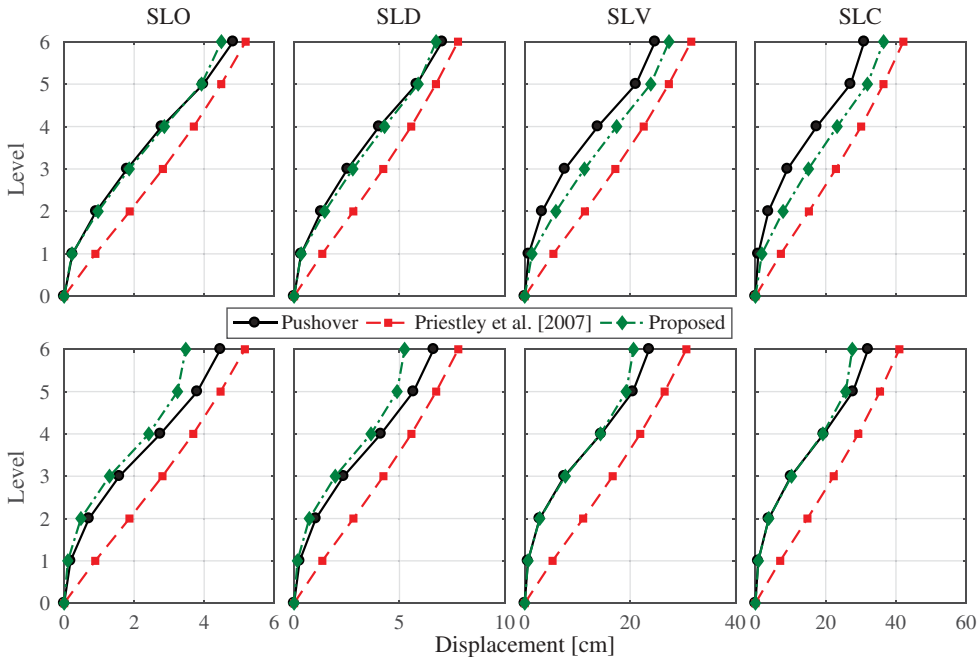


Figure 12. Comparison of the normalized displacement profiles, with different methodologies, in X (left) and Y (right) direction.

3.2.3. Application of Simplified Pushover Analysis Method

The procedure described in Section 2 was applied to the case study building in order to estimate the displacement profiles at the four limit states assessed during pushover analyses. A detailed description of the process followed for this building is provided in Saborío-Romano [2016]. In evaluating the likely mechanism, a beam-sway mechanism was predicted to develop, with sway indices all less and 1.0 (except at roof level, where column hinging would be expected) as indicated in Tables 2 and 3 for the X- and Y-directions, respectively. As such, the relative stiffnesses of different levels were first assessed and used to establish the likely displaced shape at yield and this shape was then scaled until the limit state drift was reached at the critical story. For this case study building, story drifts at the limit states SLO, SLD, SLV, and SLC were again taken as 0.33%, 0.50%, 2.0%, and 2.6%, respectively, for the X-direction and 0.33%, 0.50%, 2.0%, and

Table 2. Sway indices, displacements, and shear resistance profiles for the overall structure in the X-direction of the L'Aquila building, using the proposed procedure.

Story	Sway potential indices, S_i	Story drift average $\delta_{i,aver}$ (m)	Displacement profile Δ_i (m)	Normal displacement profile Δ_i	Shear resistance profile V_i (kN)
6	1.03	0.0067	0.0981	1.000	1334.2
5	0.44	0.0232	0.0915	0.932	936.6
4	0.32	0.0317	0.0683	0.696	1013.7
3	0.27	0.0231	0.0366	0.373	1608.3
2	0.36	0.0106	0.0135	0.138	2713.9
1	0.46	0.0030	0.0030	0.030	6379.3

Table 3. Sway indices, displacements, and shear resistance profiles for the overall structure in the Y-direction of the L'Aquila building, using the proposed procedure.

Story	Sway potential indices, S_i	Story drift average $\delta_{i,aver}$ (m)	Displacement profile Δ_i (m)	Normal displacement profile Δ_i	Shear resistance profile V_i (kN)
6	1.55	0.0140	0.1109	1.000	1619.1
5	0.77	0.0262	0.0969	0.874	1825.1
4	0.62	0.0248	0.0707	0.637	2519.5
3	0.64	0.0219	0.0459	0.414	3231.4
2	0.60	0.0184	0.0239	0.216	3745.6
1	0.53	0.0055	0.0055	0.050	7891.3

2.7%, respectively, for the Y-direction. The resulting displacement profiles for the various limit states are presented in Fig. 12 and are compared with the displacement profiles obtained from pushover analyses, as well as those predicted from Eq. (1) from Priestley *et al.* [2007].

As seen in Fig. 12, the displacement profile obtained with the proposed procedure accurately predicts the behavior of the structure, having stiffer lower stories and having a change in the form of the displacement profile between the third and the fifth story. The initial displaced shape obtained with Eq. (1b) that assumes a more traditional beam-sway mechanism typically found in newly designed structures does not give a good estimation on how this structure displaces. This is because it does not account for the relative changes in stiffness and strength along the height of the building.

In order to highlight the potential impact of adopting the different displacement profiles in Fig. 12, the equivalent SDOF displacement capacity, Δ_{sys} , was computed for each limit state and the results are reported in Table 4. The expression for Δ_{sys} is presented in Fig. 1 and requires knowledge of only the mass, m_i , and the displacement at each level, Δ_i (taken from the profiles in Fig. 12). Comparing the assessed displacement capacities for the building, it can be seen that the approach of Priestley *et al.* [2007] overestimates the displacement capacity for this building by up to 34%. In contrast, the new procedure provides considerable improvement, with smaller differences in displacement capacity estimates and the tendency to be conservative relative to the results of pushover analysis. As such, it is concluded that the new procedure offers considerable improvement over the existing simplified approach of Priestley *et al.* [2007]. It is also observed that the simplified pushover analysis approach permits the likely mechanism, resistance, and displacement capacity to be estimated with reasonable accuracy. There are, however, some limitations with the method, as will be underlined in the final conclusions.

Table 4. Equivalent SDOF displacement capacities assessed for the L'Aquila building using the displacement profiles assessed via different approaches.

	X-direction				Y-direction			
	SLO	SLD	SLV	SLC	SLO	SLD	SLV	SLC
Δ_{sys} from pushover analyses	0.032	0.048	0.174	0.235	0.034	0.049	0.178	0.226
Δ_{sys} from Eq. (1)	0.037	0.056	0.221	0.295	0.037	0.056	0.227	0.303
(% diff. pushover)	(15.7%)	(17.2%)	(27.0%)	(25.2%)	(10.9%)	(14.0%)	(28.0%)	(33.8%)
Δ_{sys} new procedure	0.027	0.040	0.159	0.212	0.032	0.049	0.198	0.264
(% diff. pushover)	(-16.7%)	(-15.6%)	(-8.6%)	(-9.8%)	(-3.5%)	(-0.8%)	(11.4%)	(16.4%)

4. Conclusions

A simplified pushover analysis method that engineers can apply with either hand calculations, or via use of a simple spreadsheet, has been proposed for RC frame structures. The simplified approach permits independent checks of outputs from structural analysis software and also helps inform engineers of the key characteristics of the structural system being assessed. The procedure described in this work builds on previous contributions in the literature. The main development to the state of the art is to provide an improved means of quantifying the displacement profile of RC frames, with account for different types of yielding mechanisms and structural configurations. Previous guidelines for the simplified assessment of RC frames relied on the use of an empirical expression for the displaced shape. The new approach put forward here starts by first estimating the initial story stiffness as the story shear resistance divided by the story yield drift, and then uses this information to compute a displacement profile at formation of a mechanism. Subsequently, the nonlinear displacement profile is attained by summing a plastic deformation profile, set as a function of the assessed mechanism, with the yield displacement profile. A step-by-step worked example is included in Appendix. Considering that force–displacement response predictions obtained from the simplified approach align closely with those obtained from rigorous nonlinear static analyses for a range of frame configurations and mechanisms, it is concluded that the proposed approach offers an effective means of undertaking simplified pushover analysis.

The methodology has been presented for low- to medium-rise RC frames prone to the development of beam-sway mechanisms, column-sway mechanisms, joint mechanisms, or combinations of these. However, the approach has not been developed or tested for other important cases, such as frames with masonry infills or frames prone to soil–structure interaction effects. In addition, there are limitations in the ability of the method to account for coupled modes of vibration or torsional sensitivity, similar to a normal pushover analysis. Nevertheless, it is considered that the approach presented in this work will generally aid engineers as a tool for checking a computer-based pushover analysis or for assessment of simple structures without the use of computer software.

Acknowledgments

The support of the RELUIS consortium is gratefully acknowledged. In addition, this project was partially supported by QuakeCoRE, a New Zealand Tertiary Education Commission-funded Centre. This is QuakeCoRE publication number 0351.

Funding

This work was supported by the QuakeCoRE [E6471_FP4_COORD2018].

References

- Antoniou, S. and Pinho, R. [2004] “Development and verification of a displacement-based adaptive pushover procedure,” *Journal of Earthquake Engineering* 8(5), 643–661. doi: [10.1080/13632460409350504](https://doi.org/10.1080/13632460409350504).

- Calvi, G. M., Magenes, G. and Pampanin, S. [2002a] "Relevance of beam-column joint damage and collapse in RC frame assessment," *Journal of Earthquake Engineering* 6(Supp(1)), 75–100. doi: [10.1080/13632460209350433](https://doi.org/10.1080/13632460209350433).
- Calvi, G. M., Magenes, G. and Pampanin, S. [2002b] "Experimental test on a three storey RC frame designed for gravity only," *12th European Conference on Earthquake Engineering*, London, UK.
- Carr, A. J. [2007] *RUAUMOKO - User Manual, Theory, and Appendices* (available online at <http://www.civil.canterbury.ac.nz/ruaumoko/index.html>).
- CSI. [2000] *SAP2000 Integrated Software for Structural Analysis and Design* (available online at <https://www.csiamerica.com/products/sap2000>).
- EN 1998-1:2004. [2004] *Eurocode 8: Design of Structures for Earthquake Resistance - Part 1: General Rules, Seismic Actions and Rules for Buildings*, Comité Européen de Normalisation, Brussels, Belgium.
- EN 1998-3:2005. [2005] *Eurocode 8: Design of Structures for Earthquake Resistance - Part 3: Assessment and Retrofit of Buildings*, Comité Européen de Normalisation, Brussels, Belgium.
- Fajfar, P. [2000] "A nonlinear analysis method for performance-based seismic design," *Earthquake Spectra* 16(3), 573–592. doi: [10.1193/1.1586128](https://doi.org/10.1193/1.1586128).
- FEMA 440. [2005] *Improvement of Nonlinear Static Seismic Analysis Procedures*, Federal Emergency Management Agency, Washington, DC.
- Freeman, S. A. [1978] "Prediction of response of concrete buildings to severe earthquake motion," *Douglas McHenry International Symposium on Concrete and Concrete Structures*, Detroit, Michigan, pp. 589–605.
- Galli, M. [2006] "Evaluation of the seismic response of existing RC frame buildings with masonry infills," MSc Thesis, IUSS Pavia, Italy.
- Glaister, S. and Pinho, R. [2003] "Development of a simplified deformation-based method for seismic vulnerability assessment," *Journal of Earthquake Engineering* 7(Supp(1)), 107–140. doi: [10.1080/13632460309350475](https://doi.org/10.1080/13632460309350475).
- Gulkan, P. and Sozen, M. A. [1974] "Inelastic responses of reinforced concrete structures to earthquake motions," *ACI Journal* 71(12), 604–610. doi: [10.14359/17694](https://doi.org/10.14359/17694).
- Hall, J. F. [2017] "On the descending branch of the pushover curve for multistorey buildings," *Earthquake Engineering & Structural Dynamics*. doi: [10.1002/eqe.2990](https://doi.org/10.1002/eqe.2990).
- McKenna, F., Scott, M. H. and Fenves, G. L. [2010] "Nonlinear finite-element analysis software architecture using object composition," *Journal of Computing in Civil Engineering* 24(1), 95–107. doi: [10.1061/\(asce\)cp.1943-5487.0000002](https://doi.org/10.1061/(asce)cp.1943-5487.0000002).
- NTC. [2008] *Norme Tecniche Per Le Costruzioni*, Ministro delle Infrastrutture (Italian Ministry of Infrastructure), Rome, Italy (in Italian).
- NZS 1170.5:2004. [2004] *Structural Design Actions Part 5: Earthquake Actions - New Zealand*, Standards New Zealand, Wellington, New Zealand.
- NZSEE. [2017] *The Seismic Assessment of Buildings: Technical Guidelines for Engineering Assessments, Part C-C2: Assessment Procedures and Analysis Techniques*, New Zealand Society for Earthquake Engineering, Wellington, New Zealand. Retrieved from <http://www.eq-assess.org.nz/new-home/part-c/c2/>
- O'Reilly, G. J. [2016] "Performance-based seismic assessment and retrofit of existing RC frame buildings in Italy," PhD Thesis, IUSS Pavia, Pavia, Italy.
- O'Reilly, G. J. and Sullivan, T. J. [2017] "Modeling techniques for the seismic assessment of the existing Italian RC frame structures," *Journal of Earthquake Engineering* 1–35. doi: [10.1080/13632469.2017.1360224](https://doi.org/10.1080/13632469.2017.1360224).
- O'Reilly, G. J. and Sullivan, T. J. [2018] "Probabilistic seismic assessment and retrofit considerations for Italian RC frame buildings," *Bulletin of Earthquake Engineering* 16(3), 1447–1485. doi: [10.1007/s10518-017-0257-9](https://doi.org/10.1007/s10518-017-0257-9).
- O'Reilly, G. J., Sullivan, T. J. and Filiatrault, A. [2017] "Implications of a more refined damage estimation approach in the assessment of RC frames," *16th World Conference on Earthquake Engineering*, Santiago, Chile.

- Pampanin, S., Calvi, G. M. and Moratti, M. [2002] "Seismic behaviour of RC beam-column joints designed for gravity loads," *12th European Conference on Earthquake Engineering*, London, UK. doi: [10.1044/1059-0889\(2002/er01\)](https://doi.org/10.1044/1059-0889(2002/er01)).
- Papanikolaou, V. K., Elnashai, A. S. and Pareja, J. F. [2006] "Evaluation of conventional and adaptive pushover analysis II: comparative results," *Journal of Earthquake Engineering* **10**(1), 127–151. doi: [10.1080/13632460609350590](https://doi.org/10.1080/13632460609350590).
- Park, R. and Paulay, T. [1975] *Reinforced Concrete Structures*, John Wiley & Sons, Ltd., New York.
- Pettinga, D. and Priestley, M. J. N. [2005] "Dynamic behaviour of reinforced concrete frames designed with direct displacement-based design," *ROSE Report 2005/02*, IUSS Press, Pavia, Italy.
- Pinho, R., Antoniou, S. and Pietra, D. [2006] "A displacement-based adaptive pushover for seismic assessment of steel and reinforced concrete buildings," *8th US National Conference in Earthquake Engineering*, San Francisco, CA.
- Priestley, M. J. N. [1997] "Displacement-based seismic assessment of reinforced concrete buildings," *Journal of Earthquake Engineering* **1**(1), 157–192. doi: [10.1080/13632469708962365](https://doi.org/10.1080/13632469708962365).
- Priestley, M. J. N. and Calvi, G. M. [1991] "Towards a capacity-design assessment procedure for reinforced concrete frames," *Earthquake Spectra* **7**(3), 413–437. doi: [10.1193/1.1585635](https://doi.org/10.1193/1.1585635).
- Priestley, M. J. N., Calvi, G. M. and Kowalsky, M. J. [2007] *Displacement Based Seismic Design of Structures*, IUSS Press, Pavia, Italy.
- Priestley, M. J. N., Seible, F., and Calvi, G. M., 1996. *Seismic Design and Retrofit of Bridges*, John Wiley & Sons, 686 pp.
- Regio Decreto. [1939] *Norme per l'esecuzione delle opere conglomerato cementizio semplice od armato - 2229/39*, Gazzetta Ufficiale, n.92 of 18-04-1940 - Suppl. Ord. n. 92, Rome, Italy (in Italian).
- Saborio-Romano, D. [2016] "Performance based and simplified displacement based assessment of infilled RC frame building in L'Aquila, Italy," MSc Thesis, IUSS Pavia, Italy.
- Seismosoft. [2014] *SeismoStruct v7.0 - A computer program for static and dynamic nonlinear analysis of framed structures* (available online at <http://www.seismosoft.com/seismostruct>).
- Shibata, A. and Sozen, M. A. [1976] "Substitute-structure method for seismic design in R/C," *Journal of the Structural Division, ASCE* **102**(1), 1–18.
- Sullivan, T. J., and Calvi, G. M., [2011] "Considerations for the Seismic Assessment of Buildings Using the Direct Displacement-Based Assessment Approach." In *Atti Del 5 Convegno Nazionale ANIDIS*. Bari, Italy.
- Sullivan, T. J., Priestley, M. J. N. and Calvi, G. M., Eds. [2012] *A Model Code for the Displacement-Based Seismic Design of Structures - DBD12*, IUSS Press, Pavia, Italy.
- Tasligedik, A. S., Akguzel, U., Kam, W. Y. and Pampanin, S. [2018] "Strength hierarchy at reinforced concrete beam-column joints and global capacity," *Journal of Earthquake Engineering* **22**(3), 454–487. doi: [10.1080/13632469.2016.1233916](https://doi.org/10.1080/13632469.2016.1233916).
- Vona, M. and Masi, A. [2004] "Resistenza sismica di telai in c.a. progettati con il R.D. 2229/39," *XI Congresso Nazionale "L'Ingegneria Sismica in Italia*, Genova, Italia (in Italian).

Appendix: Example application of the proposed procedure to a three-story RC frame with beam-sway mechanism

The proposed simplified procedure is applied to the RC frame structure illustrated in Fig. A1. The flexural strengths (referred to joint centerlines) of the structural elements are shown in Fig. A1 (on the right). It is assumed that beams and columns have enough shear strength to allow the development of plastic hinges. The flexural strengths of columns are based on gravity induced axial loads. Variations in axial load on the columns due to seismic loading can be accounted for via an iterative assessment process but this is not shown here for brevity.

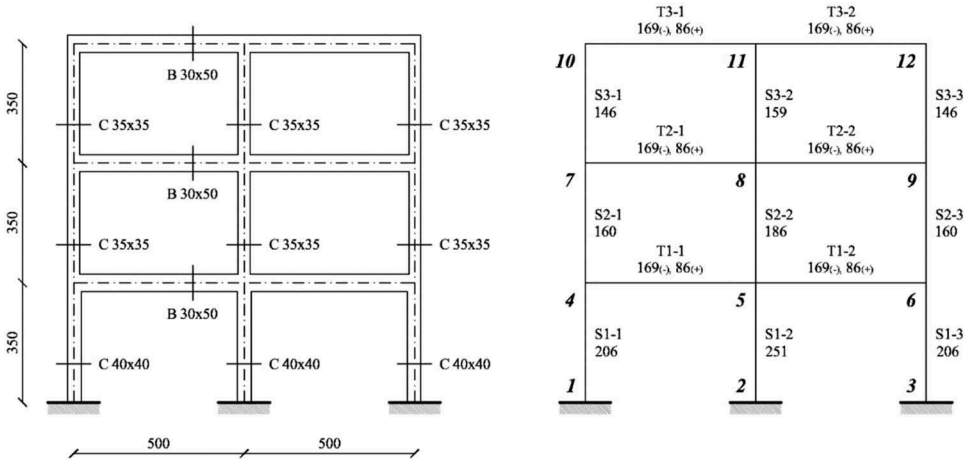


Figure A1. Geometrical dimensions in (cm) and element flexural strengths (kNm).

Assessing the likely mechanism and lateral resistance of each story: in order to assign the moments at the top and bottom part of a column, it is necessary to consider the flexural strengths that can be developed after reaching joint equilibrium. Example for node 8 from Fig. A1

$$M_{bl} + M_{br} = 169 + 86 = 255 \text{ kNm}$$

$$M_{col,b} + M_{col,a} = 186 + 159 = 345 \text{ kNm}$$

In this case (weak beam-strong column), the flexural capacity of each column (186 kNm for the column below and 159 kNm for the column above) is higher than the half of the sum of the flexural strengths of the beams (128 kNm). Hence, the moment of each column is set equal to the half of the sum of the flexural strengths of the beams (128 kNm). The values of moment obtained at the end sections of columns by evaluating the equilibrium of all nodes are shown in Table A1.

Table A1. Values of moment obtained at the end sections of columns.

Story	1				2				3			
	column	S1-1	S1-2	S1-3	Sum	S2-1	S2-2	S2-3	Sum	S3-1	S3-2	S3-3
$M_{col,b,i}$ (kNm)	43	128	85	255	43	128	85	255	86	159	146	391
$M_{col,a,i-1}$ (kNm)	206	251	206	663	43	128	85	255	43	128	85	225

The shear resistance at each story is calculated with Eq. (3) considering that the story height is the same at each story and equal to 3.50 m. For example, the second story is computed as

$$V_{R,i} = \left(\sum M_{col,b,i} + \sum M_{col,a,i-1} \right) / (h_i - h_{i-1}) = (255 + 255) / 3.50 = 146 \text{ kN}$$

The $V_{R,i}$ obtained at the third story is 185 kN, at the second story is 146 kN, and at the first story 262 kN.

Assessing the drift required to yield each story: the yield drift is calculated for each beam or column using Eqs. (4)–(10). Example for the inner column at the base level (Eqs. (9a) and (10)):

$$h_{cf} = h_1 / (M_{col,b,1} / M_{col,base} + 1) = 3.50 / (128 / 251 + 1) = 2.32 \text{ m}$$

$$\theta_{y,0} = 0.70 \varepsilon_y h_{cf} / D_{col} = 0.70 \times 0.0024 \times 2.32 / 0.40 = 0.0097 \text{ rad}$$

Table A2. Yield drift and the flexural capacities for each level.

Level	Mechanism	Node	Element	Length (m)	Depth (m)	$\theta_{y,i}$ (rad)	$M_{bl,i}$ (kNm)	$M_{br,i}$ (kNm)	$M_{col,i}$ (kNm)
3	Column	10	S3-1	3.50	0.35	0.0103	–	–	146
		11	S3-2	3.50	0.35	0.0103	–	–	159
		12	S3-3	3.50	0.35	0.0103	–	–	146
2	Beam	7–8	T2-1	5.00	0.50	0.0120	86	169	–
		8–9	T2-2	5.00	0.50	0.0120	86	169	–
		1–2	T1-1	5.00	0.50	0.0120	86	169	–
1	Beam	4–5	T1-1	5.00	0.50	0.0120	86	169	–
		5–6	T1-2	5.00	0.50	0.0120	86	169	–
0	Column	1	S1-1	2.90	0.40	0.0122	–	–	206
		2	S1-2	2.32	0.40	0.0097	–	–	251
		3	S1-3	2.48	0.40	0.0104	–	–	206

The values of yield drift and flexural capacity of the structural elements are shown for each level in Table A2, where the length is the one used in the expression of the yield drift (for level 0, the contraflexure height h_{cf}).

Once the yield drift is known for beams and columns, according to the type of mechanism at each level, it is possible to determine the system yield drift at each story with Eq. (11). An example is shown below for the second story. The obtained values for the three stories are reported in Table A3.

$$\begin{aligned} \theta_{y,sys,i} &= \frac{\sum M_{j,i} \theta_{y,i} + \sum M_{j,i-1} \theta_{y,i-1}}{\sum M_{j,i} + \sum M_{j,i-1}} = \frac{[2 \times (169 + 86) \times 0.0120] + [2 \times (169 + 86) \times 0.0120]}{[2 \times (169 + 86)] + [2 \times (169 + 86)]} \\ &= 0.0120 \text{ rad} \end{aligned}$$

Assessing values of story stiffness: the story stiffness is estimated with Eq. (16). An example is shown below for the second story. The obtained values for the three stories are reported in Table A3.

$$k_{y,i} = \frac{V_{R,i}}{\theta_{y,sys,i} h_{s,i}} = \frac{146}{0.0120 \times 3.50} = 3476 \text{ kN/m}$$

Assessing displacement and story shear profiles:

Table A3. Values of shear resistance, yield drift, and stiffness for each story.

Story	Sway mechanism at story i	$V_{R,i}$ (kN)	$h_{s,i}$ (m)	$\theta_{y,sys,i}$ (rad)	$k_{y,i}$ (kN/m)
3	Mixed (level 3: column; level 2: beam)	185	3.50	0.0112	4719
2	Beam (level 2: beam; level 1: beam)	146	3.50	0.0120	3476
1	Mixed (level 1: beam; level 0: column)	262	3.50	0.0113	6625

- Step 1. Estimate base shear at yield of frame $V_b = V_{R,1} = 262$ kN.
- Step 2. Make first estimate of displacement profile Δ_i , using Eq. (1) with $\theta_c = \theta_{y,sys,1} = 0.0113$ rad.
- Step 3. Compute set of equivalent lateral forces F_i , using Eq. (13).
- Step 4. Compute story shear demand profile V_i , using Eq. (15). Compare at each story the shear demand with the shear capacity and revise the base shear. Evaluate the ratio $V_i/V_{R,i}$ and repeat the calculation from step 3 considering a new estimate of base shear equal to the first one divided by the maximum ratio $V_i/V_{R,i}$. The previous calculations are shown in Table A4.

Table A4. Application of steps 1–4.

Story	θ_c (rad)	h_i (m)	Δ_i (m)		F_i (kN)		V_i (kN)		$V_i/V_{R,i}$	F_i (kN)	V_i (kN)	$V_i/V_{R,i}$
			Step 2	w_i (kN)	Step 3	Step 4	Step 4 final					
3	0.0113	10.50	0.1187	400	131	131	0.71	88	88	0.47		
2	0.0113	7.00	0.0791	400	87	218	1.50	58	146	1.00		
1	0.0113	3.50	0.0396	400	44	262	1.00	29	175	0.67		

- Step 5. Compute story drift components δ_i , using Eq. (15).
- Step 6. Sum drift components to identify compatible displacement profile, $\Delta_{i,comp}$, as per Eq. (16). The values from steps 5 and 6 are shown in Table A5. Compare the compatible displacements with the displacements estimated in step 2 (see Table A4). If the difference is significant, repeat the procedure from step 3 using the displacements just derived, otherwise the obtained values of displacement and story shear at first yield have been identified. The values obtained at convergence are also shown in Table A5.

Table A5. Application of steps 5– 6 and final values at convergence.

Story	V_i (kN)	$k_{y,i}$ (kN/m)	δ_i (m)		V_i (kN)	$\Delta_{i,comp}$ (m)	
			Step 5	Step 6		Step 5 final	Step 6 final
3	88	4719	0.0186	0.0870	81	0.0172	0.0850
2	146	3476	0.0420	0.0684	146	0.0420	0.0678
1	175	6625	0.0264	0.0264	171	0.0258	0.0258

Assessing the global post-yield mechanism: the sway potential index S_i is calculated to identify the most likely inelastic mechanism, using Eq. (17). An example is shown below for the second level. The obtained values for the three levels are reported in Table A6:

$$S_i = \frac{\text{sum of beam strengths at level } i}{\text{sum of column strengths at level } i} = \frac{(2 \times 169) + (2 \times 86)}{(2 \times 160 + 186) + (2 \times 146 + 159)} = 0.533$$

The obtained values of sway potential index indicate the formation of a beam-sway mechanism, with plastic hinges at the base of columns (level 0), at the ends of the beams of the levels 1 and 2 and at the top of columns (level 3). This is compatible with the results obtained in the phase “Assessing the likely mechanism and lateral resistance of each story.” In this condition, the post-yield response

Table A6. Sway potential index for each level.

Level	Sum of beam strengths (kNm)	Sum of column strength (kNm)	S_j	Sway mechanism
3	510	451	1.13	Column
2	510	957	0.53	Beam
1	510	1169	0.44	Beam

is established by assuming a fixed displaced shape derived at the first story yield (first yield point) and subsequently increasing the values of displacement until all stories have yielded.

Once the displacement profile is fixed, it is possible to calculate the drift demand θ_i at each story as $\theta_i = \delta_i/h_{s,i}$ and the story displacement ductility μ_i as $\mu_i = \theta_i/\theta_{y,sys,i}$. The story shear V_i can then be calculated using the story displacement ductility as $V_i = \mu_i V_{i,y}$. With reference to the first yield point, the ductility and story shear values are shown in Table A7.

Table A7. Determination of first point of pushover curve (yielding of the second story).

Story	Δ_i (m)	θ_i (rad)	$\theta_{y,sys,i}$ (rad)	μ_i	V_i (kN)	$M_{O/T,i}$ (kNm)
3	0.0850	0.0049	0.0112	0.439	81	284
2	0.0678	0.0120	0.0120	1.000	146	795
1	0.0258	0.0074	0.0113	0.651	171	1392

From the values of story shear, it is possible to calculate the base overturning moment $M_{O/T}$:

$$M_{O/T} = 3.50 \times 81 + 3.50 \times 146 + 3.50 \times 171 = 1392 \text{ kNm}$$

Once the effective height H_e of the equivalent SDOF system is determined (refer Fig. 1), whose result is $H_e = 8.16$ m, the base shear V_b is derived from the base overturning moment $M_{O/T}$:

$$V_b = M_{O/T}/H_e = 1392/8.16 = 171 \text{ kNm}$$

The subsequent yield points are obtained with the same procedure illustrated above for the first yield point. By increasing the values of displacement, when the ductility demand becomes larger than 1.00, the story shear remains set to the story shear resistance. The mechanism is reached when the ductility is equal or larger than 1.00 at all stories.

A comparison between the results from application of the simplified procedure (labeled DBA) and the pushover curve from SAP 2000 is illustrated in Fig. A2a. Furthermore, the normalized displacement shape obtained by applying the simplified procedure at the first yield is compared in Fig. A2b with the first mode displacement profile (1stMS) and the displacement shape at the final step of pushover analysis. Finally, Fig. A2c illustrates the distribution of plastic hinges at the final step of the pushover analysis, which corresponds with that identified previously in Table A6.

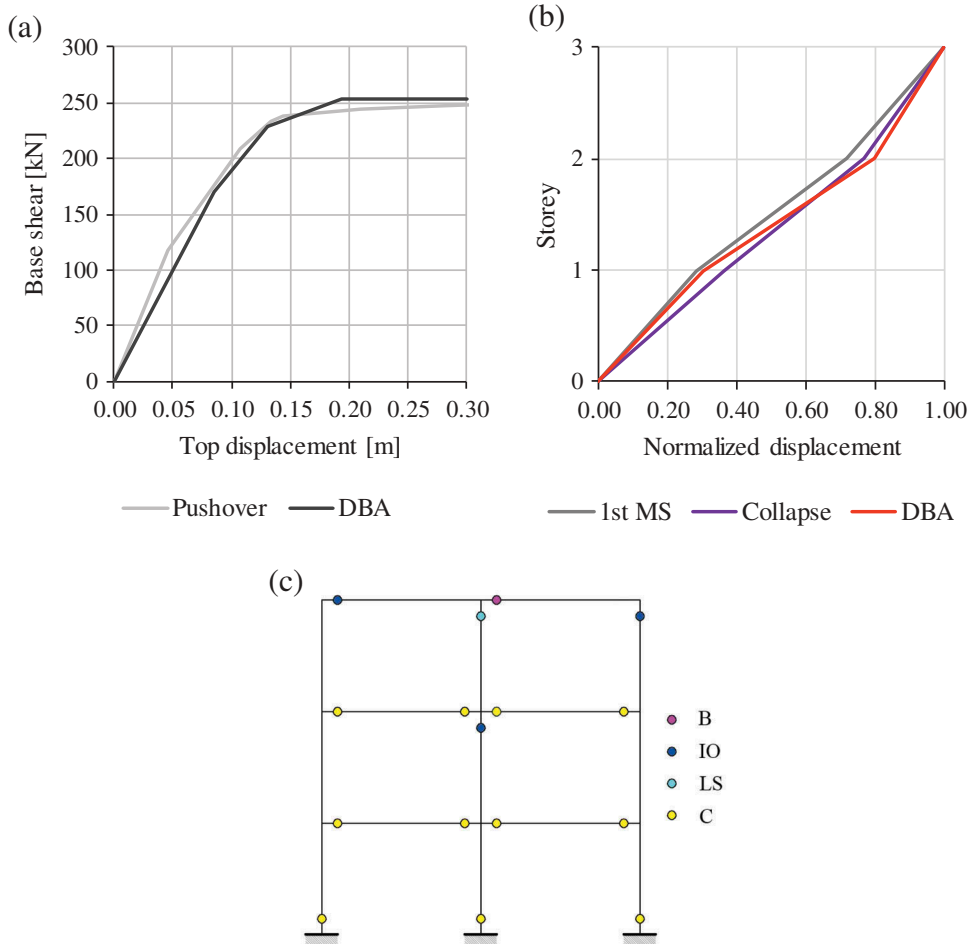


Figure A2. Comparison between pushover curve from simplified procedure and computer program (a); comparison between normalized displacement profiles (b); final configuration of plastic hinges (c).